



Contents lists available at ScienceDirect

## European Polymer Journal

journal homepage: [www.elsevier.com/locate/europolj](http://www.elsevier.com/locate/europolj)

## Macromolecular Nanotechnology

## Poly(hexamethylene terephthalate)–layered silicate nanocomposites

Nathalie González-Vidal<sup>a</sup>, Sebastián Muñoz-Guerra<sup>a,\*</sup>, Antxon Martínez de Ilarduya<sup>a</sup>, Samira Benali<sup>b</sup>, Sophie Peeterbroeck<sup>b</sup>, Philippe Dubois<sup>b,\*</sup><sup>a</sup> Departament d'Enginyeria Química, Universitat Politècnica de Catalunya, ETSEIB, Diagonal 647, 08028 Barcelona, Spain<sup>b</sup> Laboratory of Polymeric and Composite Materials (LPCM), Center of Innovation and Research in Materials and Polymers (CIRMAP), Materia Nova Research Center, University of Mons UMONS, Place du Parc 20, B-7000 Mons, Belgium

## ARTICLE INFO

## Article history:

Received 12 September 2009

Accepted 18 October 2009

Available online 22 October 2009

## Keywords:

Poly(hexamethylene terephthalate)

Masterbatch nanocomposites

Aromatic polyesters

Polyester nanocomposites

## ABSTRACT

Nanocomposites of poly(hexamethylene terephthalate) (PHT) and montmorillonite organo-modified with alkylammonium cations bearing two primary hydroxyl functions, *i.e.*, Cloisite<sup>®</sup> 30B (CL30B) were synthesized. Organoclay incorporation was performed either by dispersion in the PHT matrix via melt blending or by *in situ* ring-opening polymerization of hexamethylene terephthalate cyclic oligomers c(HT). An additional procedure combining the two methods, preparation of a highly enriched inorganic “PHT–CL30B” nanohybrid masterbatch by *in situ* ring-opening polymerization and blending of the masterbatch with additional PHT was explored. The obtained nanocomposites contain 3% (w/w) of inorganics and displayed a mixture of intercalated morphology and exfoliated nanolayers as evidenced by X-ray diffraction and transmission electron microscopy. The nanocomposite obtained by the masterbatch technique exhibited a higher degree of exfoliation and displayed slightly higher glass transition temperatures, better mechanical properties and higher flame resistance. The improved results achieved with the “masterbatch route” are a consequence of the reactions occurring between the nanocomposite constituents allowing for the grafting of PHT chains onto the organoclay surface.

© 2009 Elsevier Ltd. All rights reserved.

## 1. Introduction

The field of polymer nanocomposites is stimulating both fundamental and applied research [1–3] because these nanoscale materials are able to exhibit physical and chemical properties dramatically different from conventional microcomposites. Improvements afforded by polymer nanocomposites include increase in mechanical moduli [4–6] and heat resistance [7], decrease in gas permeability and flammability [8–12], and increase in solvent resistance, [13] as compared to the unfilled polymer. Among the potential nanocomposite formulations, those based on layered silicates have been most widely investigated, probably because the starting clay materials are easily available and because the interphase chemistry

involved in these systems had been studied for long time [14].

Polymer-layered silicate nanocomposites are prepared by incorporating finely dispersed layered silicates in the polymer matrix. Either mechanical blending of the nanoclay and the polymer or *in situ* polymerization of monomers in the presence of the layered silicates are the methods usually applied for the preparation of such nanocomposites. In general, two idealized polymer-layered silicate nanostructures are possible: intercalated and exfoliated, the greatest property changes being observed for exfoliated nanocomposites [1–3,14]. Such exfoliated structures consist of individual nanometer-thick silicate layers dispersed in a continuous polymer matrix resulting from extensive polymer penetration and delamination of the original silicate microcrystallites. However, the nanolayers are not easily dispersed in most of cases due to their preference to be face-to-face stacked in agglomerated

\* Corresponding authors.

E-mail addresses: [sebastian.munoz@upc.es](mailto:sebastian.munoz@upc.es) (S. Muñoz-Guerra), [philippe.dubois@umons.ac.be](mailto:philippe.dubois@umons.ac.be) (P. Dubois).

tactoids [15]. Intercalated hybrids characterized by a finite expansion of the interlayer silicate spacing resulting from the penetration of polymer chains into the layered silicate galleries are much more easily attainable. These consist of more or less ordered alternating polymer/silicate layers with a repeating distance of a few nanometers. In practice, many systems fall short of the idealized exfoliated morphology. More commonly, partially exfoliated nanocomposites, containing small stacks of 2–4 layers uniformly dispersed in the polymer medium, are obtained [16]. In order to improve the exfoliated structure, a new preparation technique based on the use of masterbatches has been recently developed. In this method, the nanocomposite is prepared by blending the polymer with a highly silicate-filled composite made of a premixed/dispersed polymer known to behave as a compatibilizer for the polymer matrix. Such a masterbatch strategy has been used successfully with poly(vinyl chloride) [17], chlorinated polyethylene [18–20] and poly(lactide) [21,22] along with others [23].

In the present work, the preparation, morphology and properties of nanocomposites of poly(hexamethylene terephthalate) (PHT) are investigated. PHT is a non-commercial aromatic polyester of both fundamental and applied interest that has a relatively low  $T_g$  ( $\sim 10^\circ\text{C}$ ) and moderate  $T_m$  ( $\sim 140^\circ\text{C}$ ), and that displays fair mechanical properties. As it is characteristic of aromatic polyesters, PHT exhibits an excellent chemical resistance and is not biodegradable [24]. This polyester is indeed similar to those involved in powder coating formulations [25,26]. The preparation of silicate-filled nanocomposites offers an interesting approach to obtain new materials from PHT with improved mechanical and fire resistance properties. To our knowledge only one paper dealing with these systems has been reported so far to study the effects of layered silicates on the confined crystalline morphology of PHT nanocomposites prepared by solution intercalation [27]. In the present research, we intend to ascertain the possibility of producing high-performance nanocomposites of PHT using organically modified nanoclay, specifically Cloisite<sup>®</sup> 30B (abbreviated CL30B). Two well-known preparation methods, the *in situ* ring-opening polymerization of low-viscosity hexamethylene terephthalate cyclic oligomers and direct blending of the organoclay with PHT in the melt have been comparatively applied. The main novelty afforded in this work is exploring a third method that combines ring-opening polymerization (ROP) with melt blending. A highly filled PHT–CL30B masterbatch is previously prepared and then diluted with additional amount of PHT finally offering the PHT–CL30B nanocomposites containing 3% (w/w) of inorganics.

## 2. Experimental

### 2.1. Materials

Poly(hexamethylene terephthalate) (PHT) was synthesized by conventional polycondensation of 1,6-hexanediol (HD) and dimethyl terephthalate (DMT). Hexamethylene terephthalate cyclic oligomers ( $c(\text{HT})_n$  with  $n = 2-7$ ) were

obtained by cyclo-depolymerization. These two synthesis procedures are described in full detail in the literature and here applied with minor modifications [24]. Cloisite<sup>®</sup> 30B (CL30B), an organo-modified montmorillonite containing 22% (w/w) of methyl bis(2-hydroxyethyl) tallow alkyl ammonium cations was supplied by Southern Clay Products. Tin(II) bis(2-ethylhexanoate), usually called tin(II) octoate ( $\text{Sn}(\text{Oct})_2$ ) catalyst was supplied by Aldrich, diluted with dried toluene and stored under nitrogen atmosphere. The solvents used for purification and characterization, such as toluene, methanol, chloroform and diethyl ether were high-purity grade and used as received.

### 2.2. Nanocomposite preparation by *in situ* ring-opening polymerization (ropPHT/CL30B or PHT–CL30B)

Cloisite 30B and hexamethylene terephthalate cyclic oligomers  $c(\text{HT})_{2-7}$  were previously dried overnight at  $70^\circ\text{C}$  in a ventilated oven. A mixture of CL30B (in order to reach 3% (w/w) in inorganics) in  $c(\text{HT})_{2-7}$  was used to prepare the nanocomposite. The mixture was placed in a flame-dried glass tube filled with nitrogen and added with  $\text{Sn}(\text{Oct})_2$  in a monomer/ $\text{Sn}(\text{Oct})_2$  molar ratio of 300. Polymerization was carried out for 24 h at  $160^\circ\text{C}$  under magnetic stirring. To stop the reaction, the polymerization tube was cooled down in liquid nitrogen. The recovered material was shaped as a square film (ca. 100–200  $\mu\text{m}$ -thick) by compression molding at  $150^\circ\text{C}$ . Exactly the same procedure was used to prepare the highly filled PHT–CL30B masterbatch, but using in this case a  $c(\text{HT})_{2-7}$ /CL30B mixture containing 25% (w/w) of inorganics. The masterbatch was purified by suspending the reaction mixture in chloroform followed by precipitation upon addition of diethyl ether.

### 2.3. Nanocomposite preparation by melt blending process (bdPHT/CL30B or bdPHT/PHT–CL30B)

CL30B or the PHT–CL30B masterbatch were melt blended with PHT to attain a final composition of 3% (w/w) in inorganics in a Brabender internal mixer operating at  $150^\circ\text{C}$  for 10 min at a mixing rate of 60 rpm. The collected samples were compression molded for 150 s at  $175^\circ\text{C}$  under a pressure of 150 MPa and then rapidly cooled to room temperature. For reference, PHT matrix has been processed and compressed by applying the same procedure.

### 2.4. Procedure for the clay extraction

Approximately 2 g of crude nanocomposite sample were stirred in chloroform (100 mL) for 2 h at room temperature. After centrifugation at 4000 rpm for 30 min, the supernatant was collected and the sediment solid phase was thoroughly washed by redispersion in chloroform (100 mL) followed by centrifugation, and the operation was repeated one more time. Then the supernatants were gathered, concentrated and precipitated into diethyl ether. The resulting “clay-free” polyester was filtered and dried under vacuum at  $50^\circ\text{C}$  to constant weight. The solid “clay-rich” phase was dried under vacuum at  $50^\circ\text{C}$ , to con-

stant weight. The quantity of polymer covalently grafted to the organoclay was determined by applying an extraction procedure and thermogravimetric analysis (TGA) of both the extracted solids and the residues left by the extracts.

## 2.5. Characterization

Thermogravimetric analysis (TGA) was performed under air at a heating rate of 20 °C/min from room temperature to 800 °C by using a Hi-Res TGA 2950 equipment from TA Instruments. The molecular weight of the polymer was measured by GPC using HFIP containing sodium trifluoroacetate (6.8 g/L) in a Waters equipment provided with RI and UV detectors. One hundred microliters of 0.1% (w/v) sample solution were injected and chromatographed with a flow of 0.5 mL/min. HR5E Waters linear Styragel column (7.8 mm × 300 mm, pore size 10<sup>3</sup>–10<sup>4</sup> Å) packed with crosslinked polystyrene and protected with a precolumn (VanGuard, 1.8 μm, 2.1 × 5 mm) were used. Molecular weight averages and distributions were evaluated against PMMA standards.

The morphology of the nanocomposites was analyzed by X-ray diffraction (XRD) and transmission electron microscopy (TEM). The XRD analyses were performed on a powder diffractometer Siemens D 5000 using Cu (Kα) radiation (wavelength: 0.154 nm) at room temperature in the range of 2θ = 1.5–30° at a scanning rate of 2°/min. Approximately 100–200 μm-thick nanocomposite films obtained by hot pressing were used for these analyses. TEM micrographs were recorded with a Philips CM100 instrument using an acceleration voltage of 100 kV. Ultra-thin sections of the composites (ca. 80 nm-thick) were cut at –100 °C from 3 mm thick hot-pressed plates with a LEICA ultra-cryomicrotome equipped with a diamond knife.

Differential scanning calorimetry (DSC) was carried out using a DSC Q100 apparatus of TA Instruments under a nitrogen atmosphere; DSC data are reported for the second heating run from –60 to 160 °C at 10 °C/min. Tensile properties were measured with a Lloyd LR 10 K tensile testing apparatus, at 20 °C at a constant deformation rate of 50 mm/min, using dumbbell-shaped specimens prepared from compression molded samples according to the 638 type V ASTM norm. Five specimens were tested for each

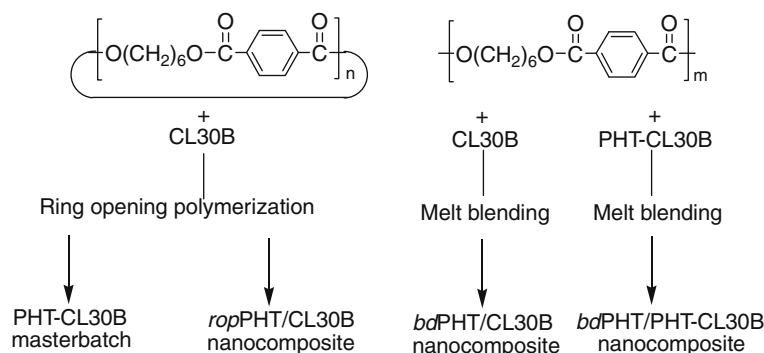
sample and the average values and standard deviations were calculated and reported. Dynamic mechanical analyses (DMTA) were performed with a DMA2980 from TA Instrument in the temperature range of –70 to 140 °C at a heating rate of 3 °C/min. Compression molded (0.5 mm-thick and 5 mm-wide) sheets of either neat PHT or PHT/CL30B nanocomposites were used. Measurements were carried out in the tensile mode at 1 Hz with a deformation amplitude of 15 μm. Fire behavior qualitative test were performed on 63 × 12 × 3 mm compression molded samples placed horizontally and simultaneously burnt starting from one extremity.

## 3. Results and discussion

### 3.1. Synthesis, composition and morphology of the nanocomposites

The different procedures applied to prepare the nanocomposites are depicted in Scheme 1. Firstly, the composition of inorganics in the nanocomposites was evaluated using TGA. The weight loss traces upon heating of neat PHT and the PHT/CL30B nanocomposites together with their respective derivative curves are shown in Fig. 1 and data are given in Table 1. The amount of residue left after heating at 700 °C in an air atmosphere revealed that nanocomposites produced either via *in situ* ring-opening polymerization or by melt blending had a content around 3% (w/w) in inorganics, which is essentially coincident with the composition used in the feed. As expected, the PHT/CL30B masterbatch left a residue of 25% (w/w) in inorganics.

An issue of high relevance in the characterization of nanocomposites is the way in which PHT is attached to the clay. Since the organoclay hydroxyl groups are able to initiate the ROP reaction, a certain amount of polymer is expected to be covalently linked to the alkylammonium tails and to be therefore ionically attached to the clay (via the hydroxyl-functionalized alkylammonium cations). To determine how much grafting of PHT on the organoclay has occurred in the nanocomposites, they were subjected to an extraction procedure with chloroform to separate the clay from the PHT matrix that is not covalently attached to the alkylammonium groups. This technique has already been successfully used to separate organoclays



Scheme 1. Schematic representation of the methodology used to prepare the nanocomposites.

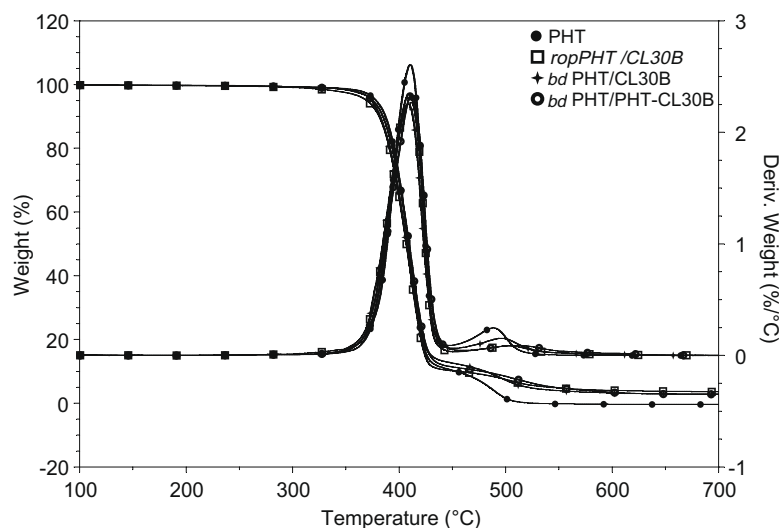


Fig. 1. Thermogravimetric traces of unfilled PHT, *rop*PHT/CL30B, *bd*PHT/CL30B and *bd*PHT/PHT-CL30B nanocomposites.

from biodegradable polymer matrices in nanocomposites [28,29]. The non-soluble organoclay settled down while the chloroform soluble PHT remained in the supernatant medium allowing for the separation of the two phases by centrifugation [29]. Fig. 2 shows the chloroform supernatant obtained from the *bd*PHT/CL30B and *bd*PHT/PHT-CL30B nanocomposites prepared by blending and from a sample of neat CL30B. No sediment was observed at the bottom of the vial after standing at any case. The supernatant was fully transparent in the case of CL30B (vial 1) and appeared fairly translucent and colorless in the case of *bd*PHT/CL30B (vial 2) indicating that no significant amount of material was dispersed in both cases. Conversely, the supernatant separated in the treatment of the *bd*PHT/PHT-CL30B nanocomposite, which was prepared using the masterbatch approach (vial 3) shows both color and turbidity indicating the presence of finely dispersed material, likely resulting from grafting of PHT on the clay via linking to the hydroxy-functionalized alkylammonium cation organo-modifier.

TGA of the solid residue left upon evaporation to dryness of the extracts was then performed. The traces recorded in this analysis are shown in Fig. 3 and data are

**Table 1**  
Molecular weight and composition of PHT and PHT/CL30B nanocomposites.

Sample	Inorg <sup>a</sup> (%, w/w)	$M_w^b$ (g/mol)	$M_w/M_n^b$	Extract <sup>c</sup> (%, w/w)	Sed <sup>d</sup> (%, w/w)
PHT	0	41,500	1.8	–	–
<i>rop</i> PHT-CL30B	3.01	34,000	1.9	0	22
<i>bd</i> PHT/CL30B	2.99	39,200	1.8	0	23
<i>bd</i> PHT/PHT-CL30B	2.96	40,700	1.8	1.9	38

<sup>a</sup> Residual weight left at 700 °C in the TGA analysis.

<sup>b</sup> Molecular weight and polydispersity determined in extracted polyester of nanocomposite.

<sup>c</sup> Residual weight of “PHT-rich” extracted phase at 700 °C in the TGA analysis.

<sup>d</sup> Weight loss between 150 and 425 °C related to the organic content of the CL30B.

compared in Table 1. The solid left by the extract obtained from *bd*PHT/CL30B totally degraded without leaving residue when heated up to 800 °C indicating that no inorganic material was present in this extract. The same analysis performed on the solid left by the extract coming from *bd*PHT/PHT-CL30B afforded a residue amounting approximately 2% (w/w) of the initial mass. The TGA analysis of the sediment phase (Fig. 3) afforded additional information on the composition of nanocomposites. The weight loss recorded between 150 and 425 °C is related to the organic content of the clay, and the analysis performed on *bd*PHT/CL30B nanocomposite gave an organic weight of about 23 wt.%, very close to the amount left by the neat CL30B which gave 22% (w/w). On the contrary, the sediment separated in the extraction of *bd*PHT/PHT-CL30B nanocomposite showed a content of 38% (w/w). This higher value of organic content in the clay phase is related to the additional amount of PHT that become linked/grafted to the organoclay by transesterification reactions. As a consequence a considerable amount of nanocomposite is enriched enough in grafted PHT as to pass into the supernatant forming a stable suspension, as observed in vial 3 (Fig. 2).

Another issue of prime importance in the characterization of the nanocomposite is the degree of dispersion attained between the two components. To assess the structure of these nanocomposites, XRD and TEM analyzes were used in combination. The powder XRD profiles of PHT, CL30B and their nanocomposites recorded within the  $2\theta$  range of 1.5–10° are compared in Fig. 4. Spacing values are calculated from the observed diffraction peaks according to the Bragg's equation. All nanocomposites prepared in this work show three peaks at approximately  $2\theta = 2.4^\circ$ ,  $5.3^\circ$  and  $7.2^\circ$ , the two formers arising from the expanded interlayer spacing of the intercalated structure (first and second order) and the latter being associated to the  $\beta$  crystal form of the PHT crystalline structure [26]. The occurrence of intercalated PHT chains into the interlayer spacing of CL30B was highlighted by a shift of the



Fig. 2. Appearance of the chloroform extract of neat CL30B (1), *bdPHT/CL30B* (2) and *bdPHT/PHT-CL30B* (3) after standing for several hours.

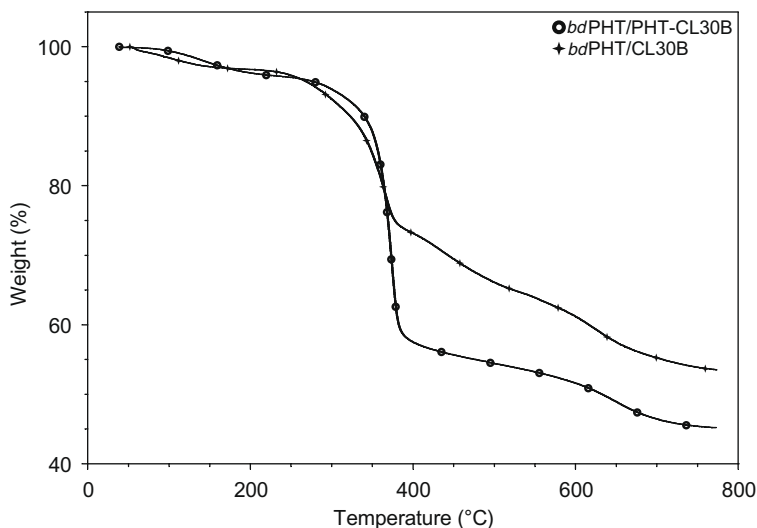


Fig. 3. TGA thermograms of the clay-enriched phase solvent-extracted from the PHT-based nanocomposites prepared by direct melt blending of CL30B and PHT-CL30B masterbatch.

peak associated to the organoclay in the nanocomposite towards lower  $2\theta$  angles. These results indicate that no complete exfoliation was attained at any case.

Complementary information on the nanocomposite structure was obtained by TEM observation of ultrathin

sections (Fig. 5). High and low magnification TEM images of *ropPHT-CL30B* nanocomposites obtained by ROP (Fig. 5a and d) show the presence of large number stacks of silicate layers and total absence of isolated sheets in the PHT matrix, confirming the exclusive presence of an intercalated structure in this preparation. Conversely, micrographs shown in Fig. 5b and e recorded from *bdPHT/CL30B* nanocomposite obtained by blending display both stacked and isolated silicate sheets indicating that an intercalated/partially exfoliated structure was generated using direct melt blending of PHT with CL30B. The existence of such stacks is responsible for the presence of the discrete scattering observed for these preparations by XRD. These stacks however are not uniformly distributed within the polymer matrix, but they appear rather grouped in populated domains erratically dispersed within the matrix. TEM images of the nanocomposite based on masterbatch *bdPHT/PHT-CL30B* (Fig. 5c and f) also shows a semi-intercalated/semi-exfoliated structure but with a fair homogeneous dispersion of exfoliated platelets and with a lesser amount of remaining stacked material. These observations reveal significant structural differences according to the preparation method used, which will be of key importance for understanding the differences in properties reported below.

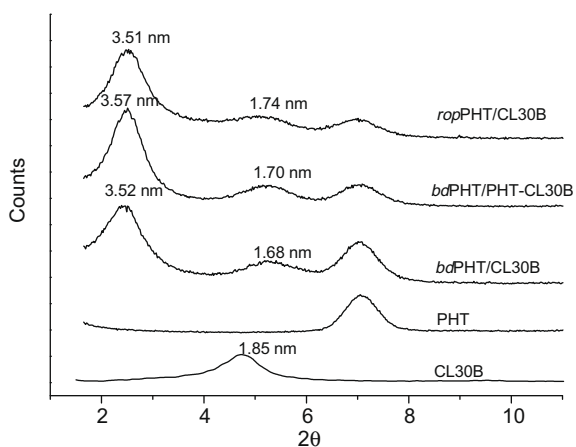


Fig. 4. Compared XRD profiles of PHT/CL30B nanocomposites obtained by *in situ* ring-opening polymerization and melt blending process.

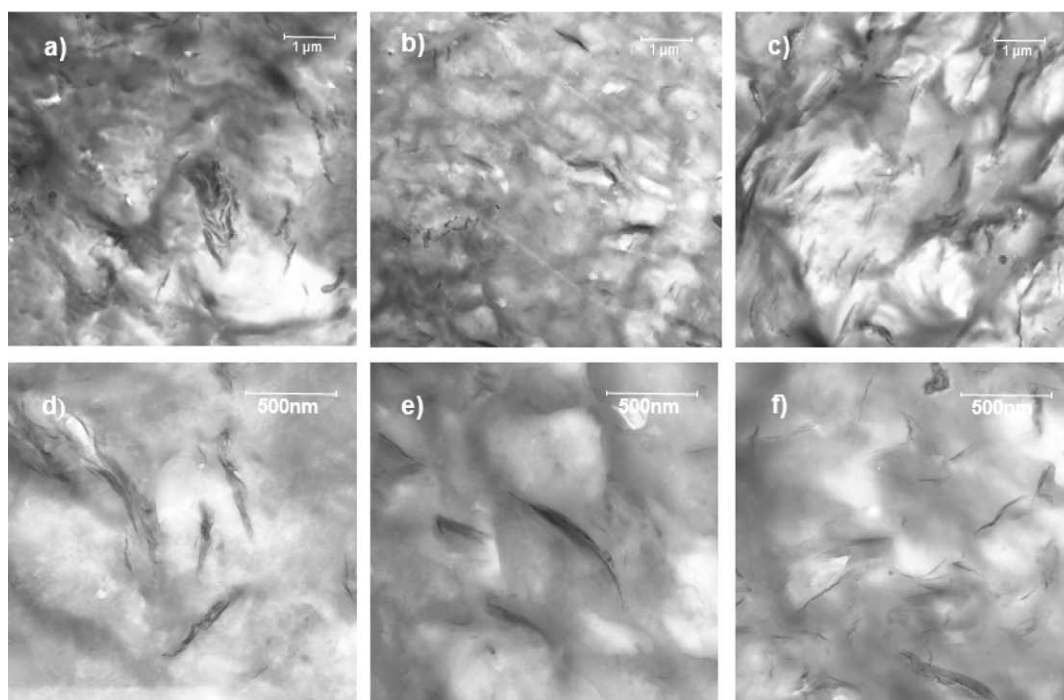


Fig. 5. TEM images of PHT/CL30B nanocomposites: (a and d) *rop*PHT/CL30B, (b and e) *bd*PHT/CL30B and (c and f) *bd*PHT/PHT-CL30B.

### 3.2. Thermal and mechanical properties of the nanocomposites

The PHT nanocomposites as well as unfilled PHT were comparatively analyzed by differential scanning calorimetry (DSC) (Fig. 6) and values obtained from this analysis are listed in Table 2. It was found that the addition of CL30B to PHT does not exert significant influence on  $T_m$  whereas  $T_g$  appeared slightly increased. On the other hand, when comparing the melting enthalpy for the nanocomposites with that of PHT, it is seen that it decreases with the addition of CL30B and hence the degree of crystallinity. This is a much expected result since it is well known that the incorporation of nanoclays in a semicrystalline polymer constitutes a physical obstacle to the molecular chain movement that hinders the crystallization process.

Also the mechanical properties of PHT nanocomposites were found to be affected by the presence of CL30B. Table 2 shows the mechanical parameters measured in tensile tests for neat PHT and two of its nanocomposites. The stress-strain curves display similar shapes for nanocomposites and the unfilled polymer indicating that the clay does not modify the overall mechanical behavior pattern of the polymer. Nevertheless, significantly higher values were observed for the Young's modulus of the nanocomposites corresponding to increase of 20–25% in the stiffness. In contrast, the elongation at break is not significantly influenced by the addition of CL30B or CL30B-PHT masterbatch. It comes out from these results that the addition of nanoclay leads to attain a significant improvement of the material rigidity while preserving ductility.

The dynamic-mechanical thermal behavior of nanocomposites was finally evaluated. The evolution of the storage modulus ( $E'$ ) with temperature for PHT, *bd*PHT/CL30B and *bd*PHT/PHT-CL30B nanocomposites was followed by DMTA analysis (Fig. 7). The interpretation of the DMTA curves should be made taking into account the mechanical reinforcement provided by exfoliated clay nanoplatelets. The storage modulus of PHT nanocomposites attained higher values than for the unfilled PHT. In the glassy state, which is present below 0 °C the modulus values of the nanocomposites did not increase significantly compared to the neat PHT matrix. Above  $T_g$ , an important increase of the moduli was observed for both composites, reaching a maximal value of 1631 MPa at 20 °C, in the case of the *bd*PHT/PHT-CL30B. The storage modulus for the nanocomposite filled with CL30B at 20 °C showed a value of 1380 MPa, which corresponds to an increase by more than 15%, whereas the nanocomposite based on PHT-CL30B masterbatch displayed an increase of almost 40%. The main conclusion derived from this dynamic-mechanical thermal analysis is that the storage modulus of PHT increases upon dispersion of nanoplatelets. This increase is larger above the glass transition temperature, because the reinforcement effect of the clay particles becomes more effective, due to the restricted movement of the polymer chains and it more apparent in the case of the nanocomposite with higher degree of exfoliation. The same effect is operating on the glass transition temperature ( $T_g$ ) in the nanocomposites, which is estimated as the maximum of  $\tan \delta$  and compared in Table 2. The addition of CL30B to the PHT matrix by blending hardly exerts influence on the  $T_g$ .

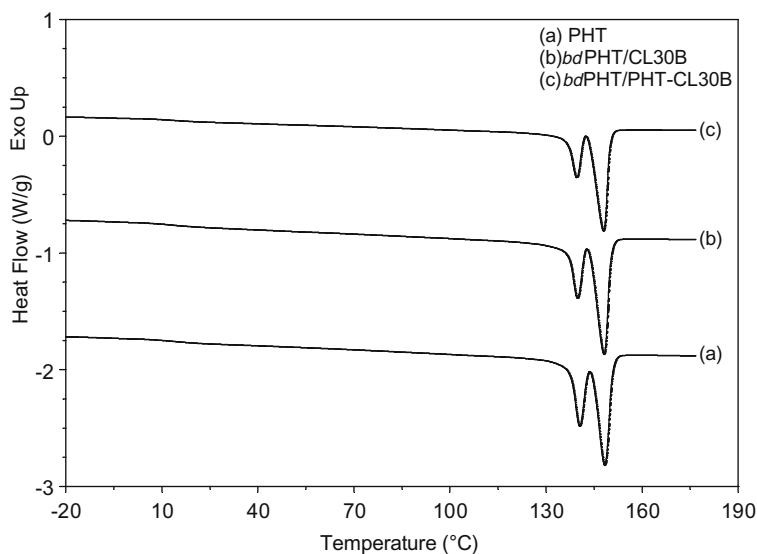


Fig. 6. Compared DSC traces of PHT and PHT/CL30B nanocomposites obtained by melt blending.

Table 2

Thermal and mechanical properties of PHT and PHT/CL30B nanocomposites.

Sample	$T_g^a$ (°C)	$T_m^b$ (°C)	$\Delta H_m^b$ (J/g)	$X_c^c$ (%)	Young modulus <sup>d</sup> (MPa)	Elongation to break <sup>d</sup> (%)	Storage modulus <sup>e</sup> (MPa)
PHT	25.3	148	44	33.7	928 ± 24	2.58 ± 0.27	1200
bdPHT/CL30B	26.4	148	39	30.3	1128 ± 43	3.46 ± 0.29	1380
bdPHT/PHT-CL30B	29.2	148	38	29.6	1137 ± 44	2.81 ± 0.49	1630

<sup>a</sup> Glass transition temperature of PHT-based materials recorded as the maximum of  $\tan \delta$  in DMTA analysis.

<sup>b</sup> Melting temperature and enthalpy determined by DSC.

<sup>c</sup> Crystallinity degree calculated on the basis of a  $\Delta H_m$  value of 144 J/g for 100% crystalline PHT [26].

<sup>d</sup> Tensile test at 20 °C at a constant deformation rate of 50 mm/min.

<sup>e</sup> Measured at 20 °C on DMTA traces obtained in the tensile mode 1 Hz (3 °C/min).

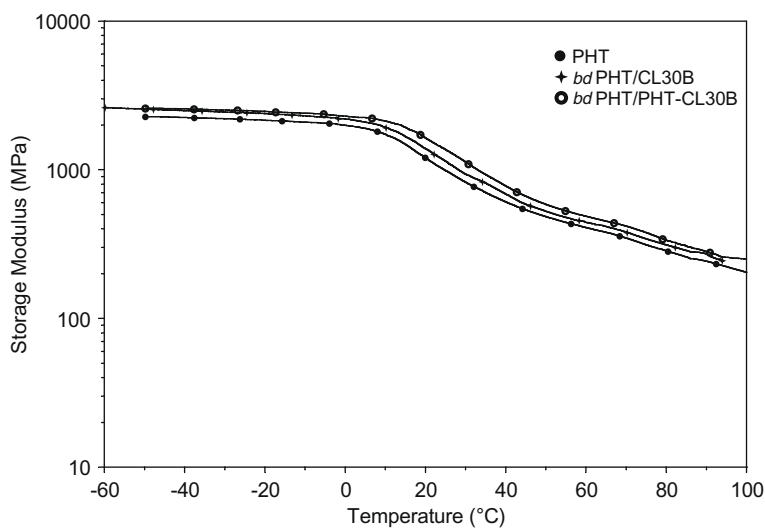


Fig. 7. DMTA traces of PHT, bdPHT/CL30B and bdPHT/PHT-CL30B nanocomposites recorded in the tensile mode.

Conversely the nanocomposite prepared by using the masterbatch exhibited a shift of the  $T_g$  from 25 up to 29 °C indicating higher restriction in the PHT chain

mobility according to a more exfoliated structure present in this nanocomposite, than in those obtained using non-grafted CL30B.

### 3.3. Fire test

The burning properties of PHT and the two corresponding nanocomposites filled with either CL30B or CL30B–PHT masterbatch were assayed by a flame visual quality test. Fig. 8 shows the burning process of specimens of PHT and the masterbatch-based PHT/CL30B nanocomposite. For the unfilled PHT, the combustion was completed after 100 s and the sample shows active bubbling/dripping during the whole process. A similar combustion behavior was observed for the nanocomposite made from CL30B via direct melt blending (not shown). On the contrary, the incorporation of PHT–CL30B masterbatch induced a dramatic change in the performance of the material. The combustion time was much longer (500 s) (Fig. 8b) and an apparent charring effect was observed for this nanocomposite at the end of the test (Fig. 8c). By half-time of the test, only one droplet had fallen down from the burning specimen

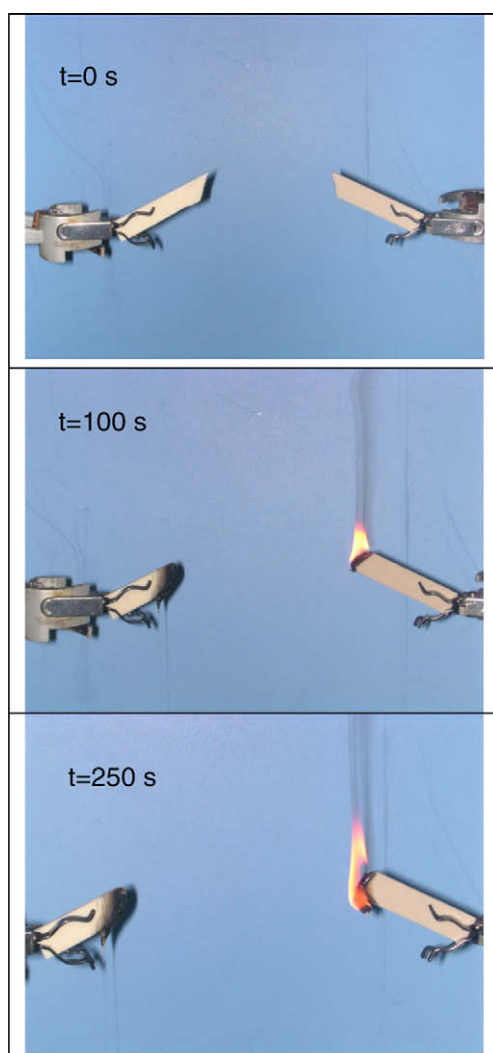


Fig. 8. Qualitative fire behavior test of unfilled PHT (left) and *bd*PHT/PHT–CL30B (masterbatch) nanocomposite (right).

and the combustion progressed preserving the shape of the original sample.

A fragile char was recovered for the masterbatch-based material while the CL30B-based composite gave the same kind of burning residue as PHT. The better cohesion of the combustion residue of the nanocomposite obtained via the masterbatch approach could be explained by the individually dispersed nanolayers forming like a supporting clay network [30]. This provides to the masterbatch nanocomposites with higher melt viscosity compared to the unfilled matrix; the char insulates the polymer from heat and slows down both the oxygen uptake and the release of volatile gases produced along the combustion. The scarce burning droplet produced during the combustion was an indication that clay exfoliation was not achieved completely on the sample. Such an increase in melt viscosity is clearly due to the presence of the effective grafting triggered by transesterification reaction between the matrix and the organoclay.

### 4. Conclusions

Poly(hexamethylene terephthalate)/layered silicate nanocomposites were prepared by dispersing Cloisite 30B into the polymer matrix by two procedures, *in situ* ring-opening polymerization of cyclic hexamethylene oligomers and melt blending of the nanoclay within the molten PHT. Partially exfoliated structures were observed for samples prepared by melt blending whereas exclusively intercalated nanocomposites could be obtained by ring-opening polymerization. In order to promote more extensive clay delamination a highly filled PHT–CL30B premix was used as masterbatch to prepare the nanocomposites. The nanocomposite containing 25% (w/w) of inorganics was obtained by *in situ* ring-opening polymerization and then blended within molten PHT yielding a nanocomposite with 3% (w/w) of inorganics. This two-step preparation method led to a nanocomposite with semi-exfoliated/semi-intercalated morphology exhibiting higher extent of clay platelet delamination. A separation procedure was applied to quantify the amount of PHT irreversibly attached to the clay. Results revealed that clay delamination was favored by the grafting of PHT chains onto the nanoclay along the blending process.

A slightly increase in  $T_g$  and a moderate decrease in melting enthalpy of PHT were observed upon addition of CL30B whereas  $T_m$  was maintained almost unchanged. Partial exfoliation of clay platelets in nanocomposites, and in a higher degree in the masterbatch nanocomposite, is responsible for the improved mechanical properties that were observed with respect to the unfilled PHT. Increases in the stiffness and storage modulus up to 20% and 40%, respectively, were attained while maintaining the elongation to break almost unchanged. Flame retardancy was analyzed by a fire visual test showing a drastically enhancement in the behavior for the case of the masterbatch-based nanocomposites. Although it should be concluded that the masterbatch approach does not lead to fully exfoliated nanocomposites, the results obtained in this work indicate that such technique could lead to a reliable easy method

to produce extensively exfoliated terephthalate polyester/clay nanocomposites with significantly improved mechanical and flame retardant properties.

### Acknowledgements

The authors thanks to the CICYT (Comisión Interministerial de Ciencia y Tecnología) of Spain for financial support (Grant MAT2006-13209-C02-02) and UMH and Materia Nova financial support from the “Belgian Science Policy” in the frame of the “Interuniversity Attraction Poles Programme” (PAI VI/27). N. González-Vidal is grateful to AGAUR for the Ph.D. grant awarded and for the “BE2007” grant in the frame of the “Beques per a estades de recerca fora de Catalunya” program.

### References

- Alexandre M, Dubois P. Polymer-layered silicate nanocomposites: preparation, properties and uses of a new class of materials. *Mater Sci Eng R* 2000;28:1–63.
- Giannelis EP. Polymer-layered silicate nanocomposites. *Adv Mater* 1996;8:29–35.
- Gorrasí G, Tortora M, Vittoria V, Galli G, Chiellini E. Transport and mechanical properties of blends of poly( $\epsilon$ -caprolactone) and a modified montmorillonite-poly( $\epsilon$ -caprolactone) nanocomposite. *J Polym Sci Polym Phys* 2002;40:1118–24.
- Giannelis EP, Krishnamoorti R, Manias E. Polymer-silicate nanocomposites: model systems for confined polymers and polymer brushes. *Adv Polym Sci* 1999;138:107–47.
- LeBaron PC, Wang Z, Pinnavaia TJ. Polymer-layered silicate nanocomposites: an overview. *Appl Clay Sci* 1999;15:11–29.
- Biswas M, Sinha Ray S. Recent progress in synthesis and evaluation of polymer-montmorillonite nanocomposites. *Adv Polym Sci* 2001;155:167–221.
- Giannelis EP. Polymer-layered silicate nanocomposites: synthesis, properties and applications. *Appl Organomet Chem* 1998;12:675–80.
- Bharadwaj RK. Modeling the barrier properties of polymer-layered silicate nanocomposites. *Macromolecules* 2001;34:1989–92.
- Messersmith PB, Giannelis EP. Synthesis and barrier properties of poly( $\epsilon$ -caprolactone)-layered silicate nanocomposites. *J Polym Sci A Polym Chem* 1995;33:1047–57.
- Kojima Y, Usuki A, Kawasumi M, Fukushima Y, Okada A, Kurauchi T, et al. Mechanical properties of nylon 6-clay hybrid. *J Mater Res* 1993;8:1179–84.
- Gilman JW. Flammability and thermal stability studies of polymer-layered silicate (clay) nanocomposites. *Appl Clay Sci* 1999;15:31–49.
- Gilman JW, Jackson CL, Morgan AB, Harris Jr R, Manias E, Giannelis EP, et al. Flammability properties of polymer-layered silicate nanocomposites. Propylene and polystyrene nanocomposites. *Chem Mater* 2000;12:1866–73.
- Burnside SD, Giannelis EP. Synthesis and properties of new poly(dimethylsiloxane) nanocomposites. *Chem Mater* 1995;7:1597–600.
- Pavlidou S, Papispyrides CD. A review on polymer-layered silicate nanocomposites. *Prog Polym Sci* 2008;33:1119–98.
- Fischer H. Polymer nanocomposites: from fundamental research to specific applications. *Mater Sci Eng C* 2003;23:763–72.
- Huang X, Lewis S, Brittain WJ, Vaia RA. Synthesis of polycarbonate-layered silicate nanocomposites via cyclic oligomers. *Macromolecules* 2000;33:2000–4.
- Lepoittevin B, Pantoustier N, Devalckenaere M, Alexandre M, Calberg C, Jérôme R. Polymer/layered silicate nanocomposites by combined intercalative polymerization and melt intercalation: a masterbatch process. *Polymer* 2003;44:2033–40.
- Benali S, Peeterbroeck S, Brocorens P, Monteverde F, Bonnaud L, Alexandre M, et al. Chlorinated polyethylene nanocomposites using PCL/clay nanohybrid masterbatches. *Eur Polym J* 2008;44:1673–85.
- Broekaert C, Peeterbroeck S, Benali S, Monteverde F, Bonnaud L, Alexandre M, et al. Chlorinated polyethylene/layered silicate nanocomposites: poly( $\epsilon$ -caprolactone)-based “masterbatch” approach. *Eur Polym J* 2007;43:4160–8.
- Brocorens P, Benali S, Broekaert C, Monteverde F, Miltner HE, Van Mele B, et al. Microscopic morphology of chlorinated polyethylene-based nanocomposites synthesized from poly( $\epsilon$ -caprolactone)/clay masterbatches. *Langmuir* 2008;24:2072–80.
- Paul MA, Alexandre M, Degée P, Calberg C, Jérôme R, Dubois P. Exfoliated polylactide/clay nanocomposites by in-situ coordination-insertion polymerization. *Macromol Rapid Commun* 2003;24:561–6.
- Paul MA, Delcourt C, Alexandre M, Degée M, Monteverde F, Rulmont A, et al. (Plasticized) polylactide/(organo-)clay nanocomposites by in situ intercalative polymerization. *Macromol Chem Phys* 2005;206:484–98.
- Urbanczyk L, Calberg C, Benali S, Bourbigot S, Espuche E, Gouanve F, et al. Poly(caprolactone)/clay masterbatches prepared in supercritical CO<sub>2</sub> as efficient clay delamination promoters in poly(styrene-co-acrylonitrile). *J Mater Chem* 2008;18:4623–30.
- Gonzalez-Vidal N, Martínez de Ilarduya A, Herrera V, Muñoz-Guerra S. Poly(hexamethylene terephthalate-co-caprolactone) copolyesters obtained by ring-opening polymerization. *Macromolecules* 2008;41:4136–46.
- David C, Lefèbvre X, Lefèvre C, Demarteau W, Loutz JM. Thermal behaviour of polyesters of hexanediol with terephthalic and isophthalic acids. *Prog Org Coat* 1999;35:45–54.
- Lefèbvre X, Koch MHJ, Reynaers H, David C. Thermal behavior of poly(hexamethylene terephthalate) oligomers I. Melting behavior and morphology of the crystalline phase. *J Polym Sci Polym Phys* 1999;37:1–18.
- Ghosh AK, Woo EM. Effects of layered silicates on the confined crystalline morphology of poly(hexamethylene terephthalate). *J Mater Chem* 2004;14:3034–42.
- Lepoittevin B, Devalckenaere M, Pantoustier N, Alexandre M, Kubies D, Calberg C, et al. Poly( $\epsilon$ -caprolactone)/clay nanocomposites prepared by melt intercalation: mechanical, thermal and rheological properties. *Polymer* 2002;43:4017–23.
- Pollet E, Delcourt C, Alexandre M, Dubois P. Transesterification catalysts to improve clay exfoliation in synthetic biodegradable polyester nanocomposites. *Eur Polym J* 2006;42:1330–41.
- Laoutid F, Bonnaud L, Alexandre M, Lopez-Cuesta J-M, Dubois Ph. New prospects in flame retardant polymer materials. *Mater Sci Eng Rep* 2009;R63:100–25.